Negative Conductivity Effects and Related Phenomena in Germanium. Part I*

Abstract: This paper is the first part of a two-part review of recent work on current instabilities and related properties of germanium in high electric fields. In this part we discuss the general subject of high field transport in n-Ge with emphasis on the concept of saturated drift velocity. The oscillations which result from bulk negative differential conductivity (BNDC) in [100] and [110] directions at low temperatures are discussed and related to the saturation effects. A discussion of theoretical and experimental evidence with regard to the BNDC effects is presented.

Finally, the anisotropy of the high-field conductivity is discussed and related to the Erlbach instability.

Introduction

The discovery of the Gunn effect¹ has stimulated a great amount of effort directed toward the production of practical solid state microwave oscillators and amplifiers, as well as a corresponding increase in fundamental studies aimed at a better understanding of the transport properties of semiconductors in strong electric fields. While the main focus of these efforts has been the direct bandgap compound semiconductors, several related instabilities have been observed in germanium in the past two years.

The instabilities discussed in this paper will be those in the microwave frequency regime ($>10^9$ Hz) which are caused by bulk negative differential conductivity (BNDC) in extrinsic material. We do not consider effects caused by minority carrier injection or by energy-dependent trapping phenomena which result in lower-frequency instabilities.

The current instabilities in Ge resulting from longitudinal BNDC are of four distinct types:

- 1) Kastal'skii and Ryvkin² have reported a Gunn effect type instability in uniaxially stressed p-Ge at 4.2°K.
- 2) McGroddy and Nathan³ reported current instabilities in n-Ge with the current in a [100] or [110] crystallographic direction for temperatures up to 130°K.
- 3) Smith⁴ has observed Gunn effect oscillations in uniaxially stressed n-Ge between 27°K and 300°K.

4) Kastal'skii and Ryvkin⁵ reported oscillations due to BNDC for temperatures below 40°K in very pure n-Ge with the current in a [111] direction.

This work has stimulated activity, both theoretical and experimental, directed toward understanding high-field transport in Ge, particularly n-type.

This review is divided into two parts. In this part we discuss the general subject of high-field transport in n-Ge. A review of work in this field up until about 1967 formed the major part of a more general treatise on high-field transport by Conwell. Only those aspects of the subject relevant to the subsequently discovered instabilities will be discussed. The second type of BNDC oscillation listed above, whose observation led to the destruction of the experimental evidence supporting the concept of a "saturated drift velocity" regime in n-Ge, is discussed in Part I. The evolution of the saturated-drift-velocity concept is discussed in some detail. This part concludes with a discussion of anisotropy effects and the Erlbach instability which arises from a transverse BNDC. In an accompanying paper,8 (referred to as II) the other three types of longitudinal BNDC oscillations are discussed, and recent work on other materials is summarized.

The region of saturated drift velocity

Ryder⁹ was the first to report successful measurement of current density j versus electric field F in a situation where the density of electrons n was kept constant, independent of field. Using the relation

^{*} Part I of this review paper was not presented at the Symposium on Instabilities in Semiconductors.

The authors are located at the IBM Thomas J. Watson Research Center, Yorktown Heights, New York 10598.

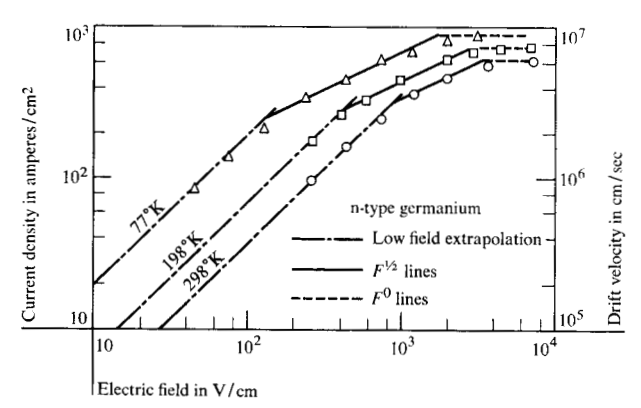
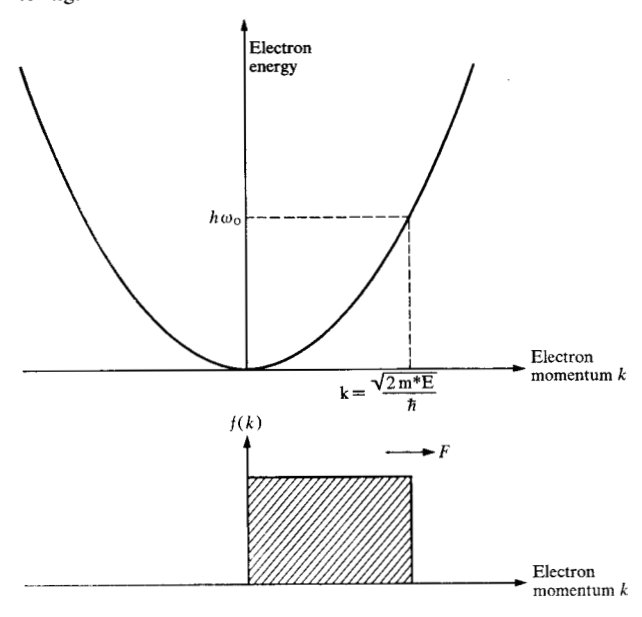


Figure 1 Current density in n-germanium as a function of electric field determined by Ryder.⁹ The drift velocity deduced from the data is shown as the right-hand ordinate.

Figure 2 (Upper) Parabolic electron energy band, with optical-mode energy indicated. (Lower) Electron distribution function for the case above with the direction of electric field indicated and extremely strong optical-mode scattering.



$$j = nev_d (1a)$$

$$= ne\mu F, \tag{1b}$$

where e is the electronic charge, he was able to determine the drift velocity v_d and the mobility μ as a function of field. Drift velocity versus average electric field as determined by Ryder is shown in Fig. 1. A linear relation between v_d and F is expected if the electrons remain in thermal equilibrium with the lattice, which is what Ryder observed at low fields. The deviation from linearity at high fields is due to the fact that the electrons are heated, i.e., they have a higher average energy than if they were in thermal equilibrium with the lattice. The straight

lines shown in this figure are from a simple model proposed by Shockley¹⁰ to interpret the data. The linear region at low fields is simply Ohm's law. Just above the linear region Ryder found a square-root region which has not been confirmed by later experiments and will not be discussed further. Finally there is the high-field region where the drift velocity is independent of field, or saturated. Ryder's data did not really clearly indicate exact saturation, but Shockley's models did predict it and, until recently, subsequent experiments were consistent with saturation.

Shockley took two extreme simplified points of view to explain the saturated drift velocity region. First, suppose that an electric field is applied as shown in Fig. 2, where we have electron energy plotted as a function of momentum or wave vector. We assume that the opticalmode scattering is very strong, so that as soon as an electron gets to the optical mode phonon energy $\hbar\omega_0$ it will be scattered back down to the bottom of the band. We also assume that the lattice temperature T is low enough so that the average energy of the electrons is small compared to $\hbar\omega_0$ at zero field and only spontaneous emission of phonons is important. Now if the electric field is high enough, the electron will absorb this energy quickly enough that the probability of scattering by another process is negligible, and we have a situation where the field excites electrons up to $\hbar\omega_0$ without any scattering, where they emit an optical phonon and scatter back to the bottom of the band. The average electron momentum $\langle p \rangle$ is equal to half the momentum corresponding to an electron energy $\hbar\omega_0$. Thus the drift velocity

$$v_d = \langle p \rangle / m^* = (\hbar \omega_0 / 2m^*)^{\frac{1}{2}}, \tag{2}$$

where m^* is the appropriate electron effective mass. The drift velocity is independent of field, so long as the field is high enough. The distribution function of electrons in momentum space is a spike along the field direction with constant density up to the momentum corresponding to an electron energy of $\hbar\omega_0$.

Such strong optical phonon scattering is not known to exist in any material. However, spiked distribution functions with carrier energies extending above the optical mode phonon energy have been shown to occur when optical mode phonon scattering is reasonably strong, as in p-type Ge. ¹¹ This phenomenon is sometimes referred to as "streaming."

The other case considered by Shockley is that in which the optical mode scattering is somewhat weaker, but still strong enough to dominate the electron energy loss. Both acoustic and optical mode scattering contribute to the momentum loss and thus determine the mobility. Yamashita and Inoue¹² have shown that when the average carrier energy $\langle \epsilon \rangle$ is much greater than $\hbar \omega_0$, the distribution

function is Maxwellian $f \propto e^{-\epsilon/kT_e}$, where $T_e = \langle \epsilon \rangle/k$ is the electron temperature). They expand the distribution function in a series of spherical harmonics and keep only the first two terms. This assumption will be discussed in more detail later. To calculate the drift velocity and electron temperature for this situation we use the energy loss method. We assume that all the electrons are at the same energy and approximately spherically distributed in momentum space (monoenergetic distribution). This is a rather severe and unrealistic approximation, but it keeps the essential points. The total rate of energy loss due to the field and collisions is equal to zero:

$$\left(\frac{\partial \epsilon}{\partial t}\right)_{\text{field}} + \left(\frac{\partial \epsilon}{\partial t}\right)_{\text{collision}} = 0, \tag{3}$$

where

$$\left(\frac{\partial \epsilon}{\partial t}\right)_{\text{field}} = e v_d F = -e \mu F^2 = -e^2 \tau_p F^2 / m^*. \tag{4}$$

 μ is given by $e\tau_p/m^*$, where τ_p is the momentum relaxation time and m^* is the effective mass in the direction of the electric field, the acceleration mass.

The rate of loss due to collisions is

$$\left(\frac{\partial \epsilon}{\partial t}\right)_{\text{collision}} = \hbar \omega_0 / \tau_0. \tag{5}$$

If $\tau_p = \tau_0$, the optical-mode scattering time, substituting (4) and (5) into (3) we find

$$\tau_p F = \text{constant} = (m^* \hbar \omega_0)^{\frac{1}{2}} / e, \tag{6}$$

and

$$v_d = \mu F = (\hbar \omega_0 / m^*)^{\frac{1}{2}}. \tag{7}$$

Again the drift velocity is independent of field in the high field limit. Saturation does not depend on the assumption that τ_p be equal to τ_0 , but only that they have the same energy dependence. Consider, for example, the case where acoustic-mode scattering contributes to momentum loss but not to energy loss. This is possible because the acoustic phonon energy is so much smaller than the optical phonon for the phonons which take part in intravalley scattering:

$$1/\tau_p = 1/\tau_0 + 1/\tau_a, \tag{8}$$

where τ_a is the acoustic mode scattering time given by

$$1/\tau_a = A_a' h \omega_a (2n+1) \rho(\epsilon) = A_a' h \omega_a (2n+1) \epsilon^{\frac{1}{2}}. \quad (9)$$

 A'_a and A''_a are independent of energy, $\hbar\omega_a$ is the acoustic-mode phonon energy, n is the Bose function given by

$$n = \frac{1}{e^{\hbar\omega_a/kT} - 1} \approx \frac{kT}{\hbar\omega_a} \tag{10}$$

and ρ (ϵ) is density of states at energy ϵ . This approximation is valid for $kT \gg \hbar\omega_a$, which is true for most temperatures. Then

$$1/\tau_a = A_a \epsilon^{\frac{1}{2}}. ag{11}$$

 A_a is independent of energy. For low temperatures and $\epsilon \gg \hbar\omega_0$, the corresponding result for optical modes is similar to Eq. (9) with n=0 (only emission is important),

$$1/\tau_0 = A_0 \epsilon^{\frac{1}{2}},\tag{12}$$

where A_0 is independent of energy. Substituting Eqs. (8), (11), and (12) into (3), (4), and (5) we find for the average energy and drift velocity

$$\epsilon = e^2 F^2 / \hbar \omega_0 A_0 (A_a + A_0) \tag{13}$$

$$v_d = \left(\frac{h\omega_0}{m^*} \frac{A_0}{A_0 + A_a}\right)^{\frac{1}{2}}.$$
 (14)

The drift velocity is saturated as before, and its saturated value is dependent on the relative values of the coupling constants for optical and acoustic modes. Comparison of Eqs. (2) and (7) shows that the values of the saturated drift velocity differ only by a factor of $\sqrt{2}$. Coupling to the acoustic modes in Eq. (14) brings the value in Eq. (7) even closer to Eq. (2). Thus, in spite of radically different assumptions about scattering rates and distribution functions, the quantity which can be determined by experiment, the drift velocity, has essentially the same behavior in the two cases. This insensitivity of experimentally observable quantities to theoretical assumptions often occurs in hot-electron problems, as, for example, in the calculation of avalanche breakdown rates. 13 In this latter case it probably accounts at least in part for the good agreement of some theoretical results with experiment.

Ryder's data, shown in Fig. 1, do not really show much in the way of saturation; the last few points at the high-field end of his velocity-field curves were, at most, consistent with Shockley's prediction of saturation. Later Gunn terported more precise measurements of drift velocity over a greater range of electric-field strengths. He observed a region between 4000 and 8000 V/cm where the velocity is saturated to within 1 per cent; at higher fields he found the drift velocity to rise again, proportional to $F^{0.134}$. This observation, along with Shockley's theoretical considerations, firmly established the concept of saturated drift velocity in n-type germanium.

Gunn's measurements were performed entirely at room temperature. More recently Nathan, ¹⁵ Barrie and Burgess, ¹⁶ and Schweitzer and Seeger ¹⁷ have reported measurements of drift velocity at both 77° and 300°K. At room temperature these results are in agreement with the notion of saturation. At 77°K nearly exact

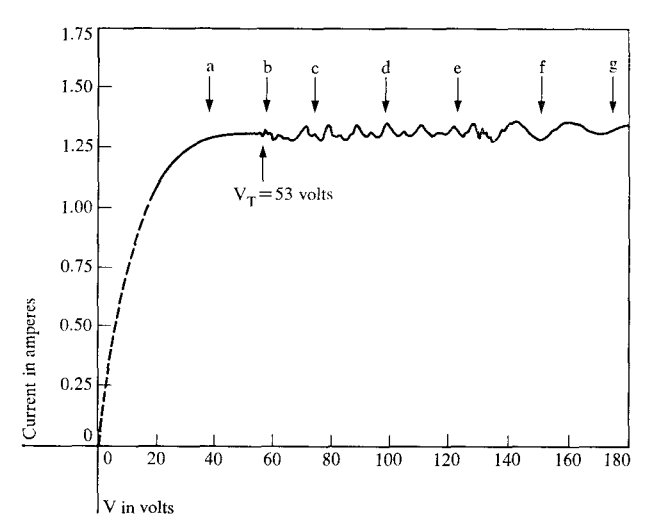
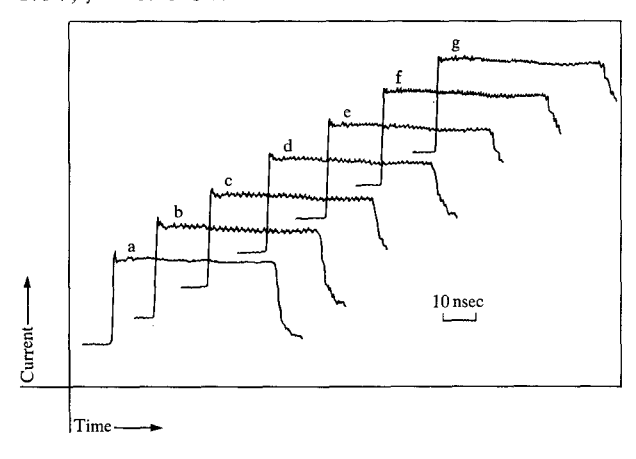


Figure 3 Current-voltage characteristic for a 0.22 mm long bar of n-Ge at 77°K. The carrier concentration is 8×10^{14} cm⁻³. The curve is measured at a fixed time after the application of the voltage pulse, using a sampling oscilloscope, and the structure above V_T is due to the voltage dependence of the phase of the current oscillations at the fixed time. The current pulse at voltages corresponding to the lettered arrows are shown in Fig. 4.

Figure 4 Time dependence of current in Sample G468 for several values of applied voltage. Values of voltage and frequently for Curves a, b... g are as follows (a) V=24V; (b) V=54V, f=0.59 GHz; (c) V=74V, f=0.65 GHz; (d) V=98V, f=0.70 GHz; (e) V=1.22V, f=0.77 GHz; (f) V=150V, f=1.35 GHz; (g) V=175V, f=1.40 GHz.



saturation was observed for currents in the $\langle 100 \rangle$ direction; in the $\langle 110 \rangle$ and $\langle 111 \rangle$ directions their results all tend towards saturation, but do not come as close as in the $\langle 100 \rangle$ case. (By this time the importance of the anisotropy of the constant energy surfaces in n-Ge had been realized, and these experiments were primarily measurements of the high field longitudinal anisotropy of the drift velocity resulting from this effective mass anisotropy. This will be discussed later at greater length).

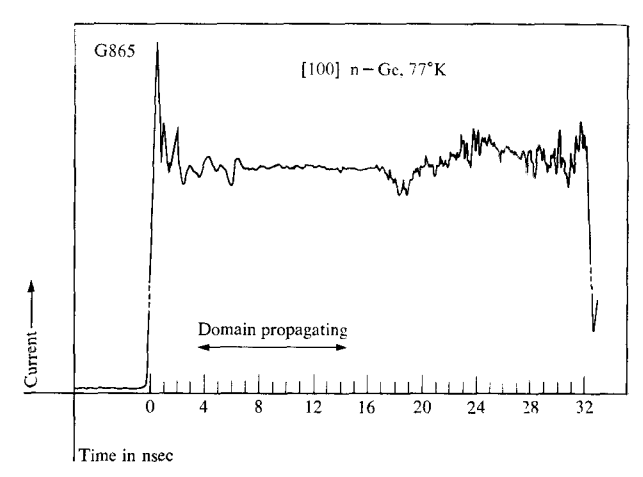


Figure 5 Time dependence of the current for "noisy breakdown" phenomenon in n-Ge. Notice that during the first few nanoseconds, corresponding to one domain transit time, the current does not increase.

In 1967, McGroddy and Nathan³ reported the existence of two types of current instabilities in this saturation region in n-Ge when the temperature was below about 120° K. The instabilities appeared when the current was along a $\langle 100 \rangle$ direction, but not when it was along a $\langle 111 \rangle$ direction. For current in the $\langle 110 \rangle$ direction the results were not reproducible.

Figure 3 shows a measurement of current density vs. average electric field at 77°K for a (100) oriented sample, 0.22 mm long, with an electron concentration of 8×10^{14} cm⁻³. The current density tends to saturate, but above about 2000 V/cm (indicated by V_T) the current starts to oscillate in time. The curve shown in the figure is measured at a fixed time relative to the beginning of the applied voltage pulses, and the structure in the curve is due to the change in the relative phase of the oscillations at that time with increasing applied voltage. The current waveform for several voltages is shown in Fig. 4. A well defined coherent oscillation can be seen for fields above threshold. The frequency of the oscillation goes through a discontinuous change at about twice threshold. At higher voltages a sudden large increase of current with voltage occurs, which usually results in a permanent change in the current-voltage characteristics of the sample.

In longer samples (l > 1 mm) a different kind of instability is observed at approximately the same field as for the type I instability discussed above, i.e., the coherent oscillations in the saturation regime. This second instability is an incoherent oscillation in the current; that is, it differs from pulse to pulse, and it appears as noise on a sampling scope, as can be seen in Fig. 5. Measurements with a traveling-wave oscilloscope indicate that this second instability (which we call type II) has frequencies in the range of 10^8 Hz.

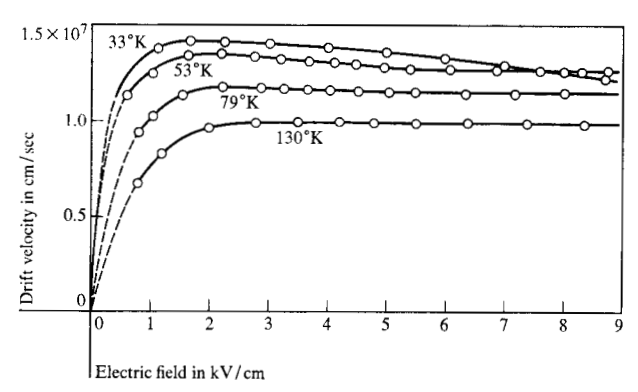


Figure 6 Velocity-field characteristic of electrons in Ge determined by transit-time measurements on reverse biased i-n⁺ diodes (Chang and Ruch).

It was not immediately evident what the explanation for these instabilities was. However, a phenomenological explanation was provided shortly thereafter and verified by experiments of Elliot, Gunn, and McGroddy¹⁸ and Chang and Ruch¹⁹ which showed for the (100) orientation a bulk negative differential conductivity begins approximately at the threshold field for the instabilities.

As we discuss later, measurements of current vs voltage where there is BNDC made by ordinary techniques do not give the true current density vs electric field because a uniform field is unstable and the field becomes non-uniform. This phenomenon can be avoided if measurements are made in a time less than the dielectric relaxation time. Figure 6 shows the results of Chang and Ruch, who measured the time-of-flight of pulses of electrons across a Schottky barrier. It can be seen that BNDC is observed for temperatures less than about 130°K (as are the instabilities), and its magnitude increases with decreasing temperature.

The presence of BNDC means that a situation exists similar to that which occurs in the Gunn effect in GaAs and several other compound semiconductors. Traveling domains characteristic of the Gunn effect are expected. Indeed such domains have been observed at 27°K where the BNDC effect is relatively strong, as indicated in Fig. 7. Here, current vs time is shown. The increases in current correspond to the annihilation of the domain at the anode and the formation of a new domain at the cathode, which then travels down the sample during the rest of the cycle.

However, the properties of the coherent oscillations seen at 77°K are quite different from the usual Gunn effect oscillations. For example, the frequency is never so low as would be expected from electron transit times, and the frequency, as discussed above, changes discontinuously with applied voltage. We see however from Fig. 6, that the negative conductivity is extremely weak at 77°K, so that one might expect the gain to be insufficient to get well formed domains. McGroddy²¹ has



Figure 7 Current waveform, showing spikes associated with travelling domains for a sample of n-Ge at 27° K biased by a pulse of 52 V amplitude. Sample length is 190μ and the horizontal scale is 2 nsec per major division. (Elliott, Gunn and McGroddy).

capacitively probed germanium samples while they were oscillating. He finds that there are disturbances or space-charge waves propagative down the sample at the electron drift velocity. The shape of waves is not constant, however. They appear to grow as they go from the cathode to the anode. Often only a portion of the sample is active. This kind of behavior is to be expected in samples with small gain

With the capacitive probe McGroddy²¹ has also studied longer samples, in which the type II instability is observed. He finds that this instability is caused by impact ionization in the domain of electron-hole pairs across the energy gap. Figure 8 shows McGroddy's capacitive probe data for a long sample which exhibits impact ionization. $\partial V(x, t)/\partial t$ (the time derivative of potential) is plotted as a function of distance along the sample for successively longer times after turn on of the voltage pulse. The regions of high $\partial V/\partial t$ correspond to a high-field region.

The motion and growth of the high-field region or domain from the cathode to the anode can be seen. The appearance of a noisy region behind the domain can be seen toward the end of the sequence after the field in the domain has had time to build up to a large value. The noise is apparently due to fluctuations in the generation rate of electron-hole pairs in the domain. The presence of excess electron-hole pairs has been verified by double pulse experiments. 16,22 Two successive voltage pulses are applied to the sample in rapid succession (separated by a few nanoseconds). The second pulse serves as the probe and is always smaller than the threshold voltage for the noisy instability. If the first pulse is also below the threshold, the current during the second pulse is independent of the magnitude of the first pulse. If the first pulse is greater than threshold, the current driving the second pulse is initially higher, showing the presence of excess electron-hole pairs. The current decays back to its original value as the holes are swept out of the sample.

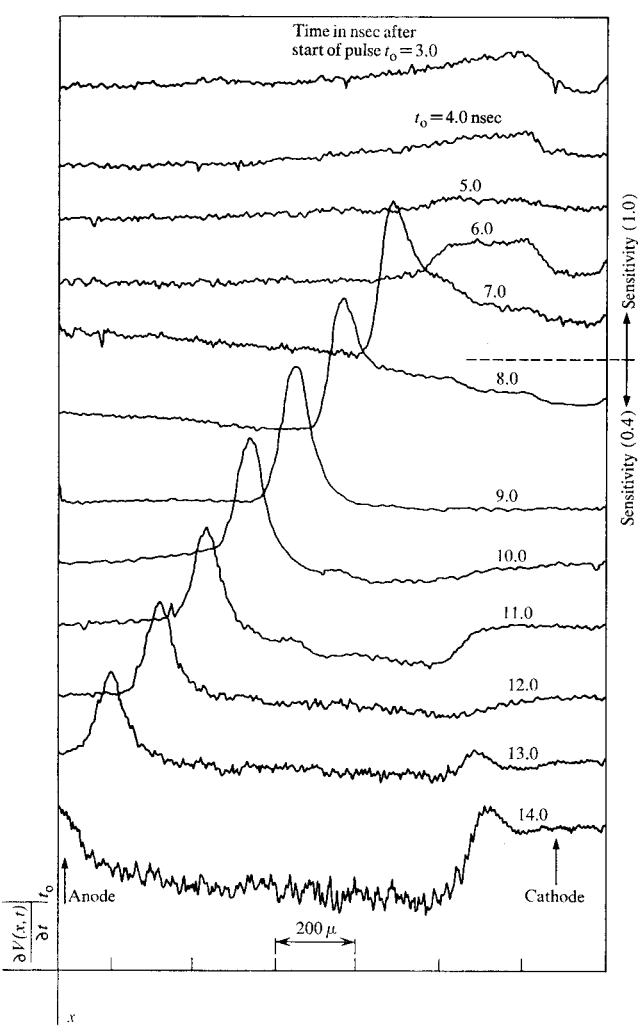


Figure 8 Capacitive probe measurement of domain motion preceding "noisy breakdown" in n-Ge at 77° K. Sample length is 1.22 mm and doping is 8×10^{14} cm⁻³. The ordinate is $-\partial V(x, t)/\partial t|_{t_0}$, the time derivative of the sample voltage at point x at time t_0 . The abscissa is position x. Successive traces correspond to value of t_0 increased by 1 ns and correspond to successive frames of a motion picture. The high-field domain which originates near the cathode, grows over a distance of several hundred microns (Note the scale change after 7 nsec). When the peak field in the domain becomes sufficiently large, electron-hole pairs are produced within it and propagate (noisy region) toward the cathode. The anode is grounded in this sequence and V(x, t) is measured with respect to ground.

The instability reported by Heinrich and Ferry²³ is probably of this type. The dimensions of their samples are large enough. Their current-voltage characteristics show an increase in current above the saturation value indicating the presence of electron-hole pairs. One can see how low frequency (lower than that implied by the transit time) oscillations can result from this instability in the following way: First a domain travels across the

sample, leaving a trail of excess electron-hole pairs in its wake. These excess pairs prevent the nucleation of a new domain. However, the holes are mobile and are subsequently extracted to the cathode. After this extraction process, the cycle can repeat if proper circuit conditions are provided. It is a type of relaxation mode.

One question connected with these phenomena comes to mind: With the many measurements of the high-field conductivity of Ge in the fifties and early sixties, why were the instabilities not observed until 1967? In fact there are several reports of "breakdown" phenomena in the literature, which are probably related to these instabilities. Barrie and Burgess¹⁶ reported a breakdown effect which is probably related to the instability that produces type II oscillations reported by McGroddy and Nathan. Jørgensen, Meyer and Schmidt-Tiedemann²² reported similar breakdown effects which they attributed to the surface. In any case, the "breakdown" effects could be eliminated by using a sufficiently low electron concentration or by orienting the current away from $\langle 100 \rangle$. The coherent type I oscillations were probably not detected earlier because the frequencies involved (>1 GHz) are well above the passband of typical equipment which had been used before sampling oscilloscopes became widely available. The exact saturation effects which were observed at temperatures below 120°K were in fact a consequence of the negative conductivity, as had been shown by Shockley.20

We now discuss this effect. With the exception of several microwave conductivity measurements²⁴ which lack the sensitivity for detection of small BNDC effects, the earlier experiments all have one thing in common. The quantities actually measured were current and voltage in a sample of appropriately oriented n-Ge with electrical contacts which injected no minority carriers. It was assumed that the electric-field strength was uniform, and that the drift velocity and current were simply proportional, to deduce the velocity-field curves from the measured current-voltage characteristics. However, Shockley²⁰ showed in the presence of a BNDC effect this procedure is not valid. His results demonstrate that when the boundary conditions were properly taken into account, the existence of a BNDC effect is not observable in the dc current-voltage characteristic-in fact, for a sufficiently long sample, in the absence of instability, the existence of BNDC leads to a "saturated" I-V characteristic.

Consider a sample of length l and equilibrium current carrier density n_0 with thin, heavily doped contacts at both ends. Neglecting diffusion, the current density, which is independent of position x, is given by

$$j = n(x)ev_d(F), (15)$$

and Poisson's equation is

$$\frac{dF}{dx} = \frac{[n(x) - n_0]e}{\epsilon},\tag{16}$$

where n(x) is the carrier electron concentration and ϵ is the dielectric constant. Eliminating n(x) from (16) by using (15) we obtain an explicit relation for dF/dx:

$$\frac{dF}{dx} = \frac{n_0 e}{\epsilon} \left(\frac{\bar{v}}{v_d(F)} - 1 \right),\tag{17}$$

where $\bar{v} = j/n_0 e$ is the velocity with which n_0 carriers must move to carry current density j.

Suppose the velocity-field curve of the sample material is as shown in Fig. 9a, having weak BNDC above a threshold field. Consider currents j_1 and j_2 , corresponding to the values \bar{v}_1 and \bar{v}_2 shown in the figure. Letting x=0be the cathode, where the boundary condition (i.e. the heavily doped contact) requires that F = 0, we find for $\bar{v}_1 < v_{\text{max}}$ that at $x = 0 \ dF/dx$ diverges, but decreases such that at $F = F_1$ we have $v(F_1) = \bar{v}_1$. The distance over which this variation occurs is of the order of $\epsilon F_1/n_0 e$. The resulting dependence of F on position F(x) is shown in Fig. 9b. For $j_2 = n_0 e \bar{v}_2$ we can see from Eq. (17) that dF/dx never reaches zero, since $\bar{v}_2 > v_{\text{max}}$, and so dF/dxis always positive. There is an inflection point in F(x)at the threshold field F_t , and above F_t the field rises rapidly with x. Examination of (17) shows that, for any point x, F(x) is an increasing function of x and that if the sample length and carrier density satisfy

$$n_0 l > \epsilon F_t / e, \tag{18}$$

the current density will rise only very slightly with increasing voltage once $j > n_0 e v_{\text{max}}$.

The current-voltage characteristic associated with a velocity-field curve such as shown in Fig. 9a, when Eq. (18) is satisfied, is shown in Fig. 10. The essential feature is that the current-voltage characteristic for a sample with such a velocity-field curve saturates at $j_{\text{sat}} = n_0 e v_{\text{max}}$.

It is clear, in view of Shockley's analysis, that at least below $T=120\,^{\circ}\mathrm{K}$ the saturation effect observed for current along [100] or [110] directions is a consequence of the existence of BNDC. In fact the background field distribution on which the travelling waves responsible for the coherent oscillations are superimposed has just the form shown in Fig. 9b. The field is lowest near the cathode and highest near the anode for a uniform sample.

Recent measurements²⁵ of the high-field conductivity at 300°K can be interpreted in terms of a positive differential conductivity for $\langle 100 \rangle$, $\langle 110 \rangle$ and $\langle 111 \rangle$ current directions at all fields below 30,000 V/cm, in agreement with the results of microwave measurements.⁶ However, when the absolute value of the slope of the velocity-field curve is small, i.e., when it is nearly saturated, it is not in general possible to deduce the magnitude or even the sign of this slope from the results of current-voltage

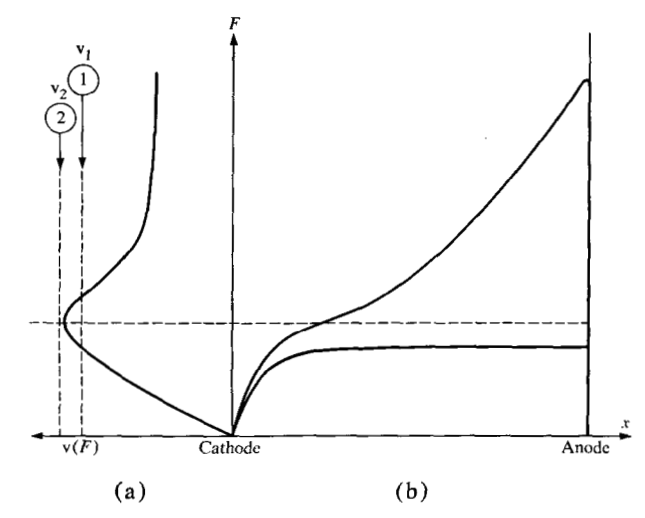
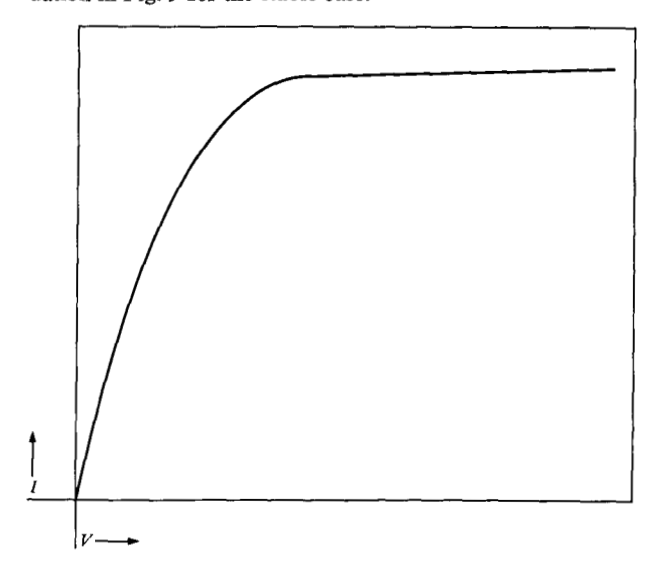


Figure 9 (a) Typical BNDC dependence of electron drift velocity on field. (b) Resulting spatial dependence of electric field for two current densities indicated in (a).

Figure 10 Current-voltage characteristic resulting from situation in Fig. 9 for the stable case.



characteristics because small nonuniformities of the sample produce gross nonuniformities in the electric-field distribution. In a sample in which the electric field was measured to be essentially uniform in an average field of 3000 V/cm, the field as a function of position was found to deviate from its mean value by as much as 25 percent when the average field was 7000 V/cm. ^{25a}

Thus the question of the existence of a weak positive or negative slope to the velocity-field curve at room temperature is still open. At low temperatures ($T \lesssim 120^{\circ}$ K) it is clear, however, that the experimental basis for the

concept of a saturated drift velocity at high field strengths is an incorrect interpretation of experimental data, i.e., inferring saturation of the velocity field curve from saturation of the corresponding current voltage characteristic. What about the various theoretical bases? Shockley's considerations, as well as subsequent theoretical efforts, 6 have all been based upon essentially a single valley model of the conduction band of germanium. The four (111) valleys lying lowest in energy are treated essentially as one parabolic band, and the higher-lying (000) and $\langle 100 \rangle$ valleys are completely ignored. The $\langle 000 \rangle$ valley lies 0.14 eV above the (111) valleys; however it has very low effective mass and density of states, so it is probably reasonable to ignore its contribution to highfield transport. In the past the assumption has been made that the $\langle 100 \rangle$ valleys, lying 0.18 eV above the (111) valleys, 26 are too far removed in energy to be appreciably occupied and to be involved in transport. Paige,²⁷ Jørgensen, Meyer and Schmidt-Tiedemann²² and others have in the past suggested that this might not be true, that is, when the electron velocity is in the "saturation" regime, the average electron energy, given by Eq. (13) for example, is sufficiently large that the higher lying minima must be appreciably populated.

In order to determine the role of these upper minima, particularly the (100) minima, in the BNDC effect the effects of uniaxial stress²⁸ and hydrostatic pressure²⁹ on the oscillations have been studied. Compressive uniaxial stress was applied on a {100} face of a sample at 27°K and current flow was along a (100) direction either normal or parallel to the stress direction. Application of the stress lowers the pair of (100) minima with their axes of symmetry along the stress direction relative to the (111) minima, which remain degenerate. The $\langle 000 \rangle$ minimum as well as the other two pairs of $\langle 100 \rangle$ minima are raised in energy relative to the $\langle 111 \rangle$ minima. The intuitively anticipated result, if transfer to the $\langle 100 \rangle$ minima is responsible for the BNDC effect, is that the application of moderate stress, either transverse or longitudinal, should decrease the threshold field for the instability—although the removal of the degeneracy of these $\langle 100 \rangle$ minima introduces an additional complication. In fact it was found that just the opposite occurs—lowering one pair of $\langle 100 \rangle$ minima relative to the $\langle 111 \rangle$ minima raises the threshold field. The increase in threshold field is approximately quadratic in the magnitude of applied stress, and the effect is twice as large for transverse stress as it is when the stress and current are parallel. Although the experimental results are opposite to what one might expect for an intervalley transfer type of BNDC, the fact that the energy position for the (100) minima affects the threshold field indicates that their role is not negligible.

In order to eliminate the unwanted complication of splitting the $\langle 100 \rangle$ minima, measurements were made

of the effects of hydrostatic pressure on the oscillations at 77°K. With increasing hydrostatic pressure the energy separation between the $\langle 100 \rangle$ and $\langle 111 \rangle$ minima is reduced and a pressure of about 30 kilobars²⁶ is sufficient to reduce this energy separation to zero. Here the anticipated result for an intervalley type of BNDC effect would be that the threshold field would decrease with increasing hydrostatic pressure up to pressures of approximately 25 kilobars, where thermal occupation of the $\langle 100 \rangle$ minima would begin to be important. Above that pressure, the oscillations would disappear. (In fact it was just such considerations and their experimental verification30 which provided convincing evidence for the intervalley transfer mechanism in n-GaAs.) Again the actual result is quite different. As pressure is applied, the threshold field rises and the amplitude of the current oscillations decreases, until at a pressure of 4.1 kilobars the oscillations disappear altogether. At this point the $\langle 111 \rangle - \langle 100 \rangle$ separation has been reduced only by about 15 percent, and thermal occupation of the (100) minima is still negligible at 77°K. Both of these pieces of evidence suggest that increasing the transfer into $\langle 100 \rangle$ minima is deleterious to the instability. That the (100) minima are not appreciably occupied up to and just below the threshold field at 77°K may be deduced from the following fact: application of a pressure of 10.5 kilobars, more than twice that sufficient to suppress the oscillations entirely, has only a few percent effect on the I-V curve below 2300 V/cm, the threshold field at atmospheric pressure at 77°K. These effects of varying the positions of the relevant bands have not been reproduced by any of the models which we discuss below.

On the other hand, considerations³¹ of the threshold field for oscillations in strained n-type germanium, which are discussed in more detail in II, lead one to conclude that these upper minima must be appreciably occupied in the field range of the BNDC discussed here. With the aim of explaining the negative conductivity effects, more realistic calculations have recently been undertaken. Dumke³² has used a model which neglects the higher lying minima, but includes the proper phonon distribution function, i.e., it does not assume classical excitation of the acoustic modes as in Eq. (10). He also includes the effect of nonparabolic bands. Although numerical calculations based on this model, using appropriate coupling constants, does indicate the existence of an in-band negative conductivity at sufficiently high electric fields, the average carrier energy in the negative conductivity region is again too large for the (100) minima to be ignored.³² Price³³ has performed similar calculations for parabolic bands. For the more special case when the form of the energy distribution function is determined by electron-electron interactions, Stratton³⁴ had shown that even with a parabolic band, at high

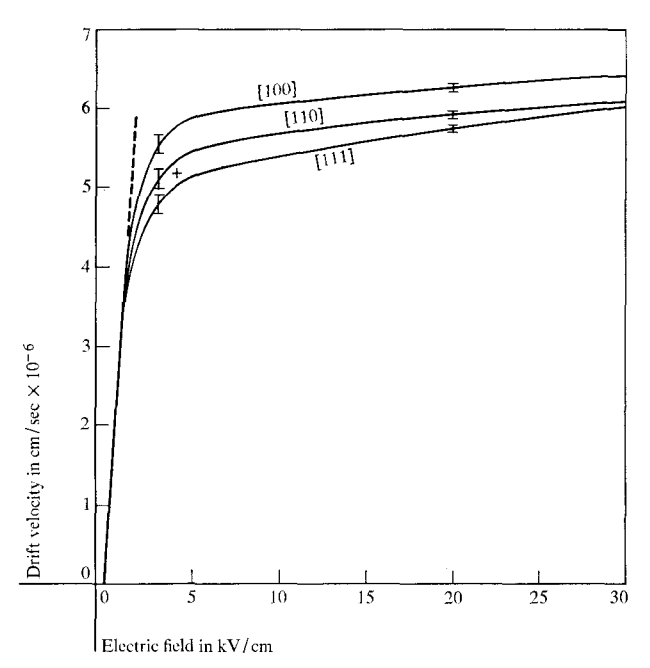


Figure 11 Dependence of electron drift velocity on field for high-symmetry directions at 300°K after Smith.²⁵

electric fields $v(F) \propto F^{-1/3}$ for mixed acoustic and non-polar optical-mode scattering. Fawcett and Paige 35,36 have done Monte Carlo calculations on a model which incorporates the $\langle 100 \rangle$ minima. However, in this model, equipartition of the phonon distribution is assumed, and the nonparabolicity of the $\langle 111 \rangle$ valleys is not included. The properties of the $\langle 100 \rangle$ minima are scaled from silicon parameters, and the inequivalent ($\langle 111 \rangle \leftrightarrow \langle 100 \rangle$) intervalley scattering coupling constant is taken as an adjustable parameter. With an appropriate choice of this parameter, this model is in reasonable agreement with experiment. To our knowledge, a Monte Carlo calculation incorporating the nonparabolicity of the $\langle 111 \rangle$ minima and the nonequipartition of the acoustic phonons has not yet been performed.

Anisotropy

In 1955 Shibuya³⁷ pointed out that because the lowest germanium conduction band is not spherically symmetric, but has ellipsoidal constant energy surfaces in k-space centered on the $\langle 111 \rangle$ Brillouin zone faces, the high-field conductivity is expected to be anisotropic. If the electric field is not along a two-, three- or four-fold rotation axis, the electric field will in general not be parallel to the current. Thus in the usual experimental method, namely sending a current through a bar of semiconductor and measuring the potential drop along the bar, there will be a transverse field. This effect has been observed by Sasaki and co-workers.³⁸

For the current along a rotation axis the field may be parallel to the current, although this solution may not be unique, as we discuss later. However the shape of the current-voltage characteristic still depends on the current direction. ^{15,16,22,25,39} At room temperature this longitudinal anisotropy is still present but considerably reduced from its magnitude at 77°K. ^{25,39} Recent room temperature results are shown in Fig. 11.

Quantitative fits of the drift velocity, its anisotropy and the transverse anisotropy, as a function of field were performed by Reik and Risken, 40 giving good agreement with experiment. Their model assumes a nearly spherical distribution function and predicts that when the mean electron energy is large compared to the optical mode energy $\hbar\omega_0$, the electron temperature T_e is proportional to F^2 . This is essentially the same assumption that leads to Eq. (13). As we have seen earlier, however, there is really no range of fields for which this model is applicable, because if the above assumption about the average electron energy is satisfied, the higher lying conduction band minima are appreciably occupied and cannot safely be ignored. The situation for fields applied along directions other than (100) is further complicated by the different average electron energies in the various valleys.

Erlbach effect

For the moment we ignore these difficulties. The calculations of Reik and Risken suggest that for current directions near the two-fold axes, the $\langle 110 \rangle$ directions, field direction is a triple-valued function of current direction. The situation where field and current are parallel is merely one of the three allowed field directions for $\langle 110 \rangle$ current. Erlbach⁷ has shown that if the equivalent intervalley scattering rate is high enough, the situation in which the $\langle 110 \rangle$ current and field are parallel is unstable. This may be readily understood by analysis of the simplified model shown in Fig. 12. The x direction is a symmetry axis for the two anisotropic valleys shown. If an electric field is applied in the x direction, the current, given by

$$\mathbf{j} = \sum_{\nu} n_{\nu} e \left(\frac{\overleftrightarrow{\tau}_{\nu}}{m_{\nu}} \right) \cdot \mathbf{F} \tag{19}$$

is also in the x-direction, because the contributions to the y-component of current by the two valleys (indicated by the index ν in Eq. (19) are equal in magnitude and opposite in direction, and so cancel. Now suppose the field is slightly off the x-direction and given by

$$\mathbf{F} = F_x \hat{\mathbf{x}} + F_y \hat{\mathbf{y}}, \tag{20}$$

with $F_x \gg F_y$. Now to first order there will be two contributions to j_y , the y-component of the current: First there will be j_{yy} , the contribution due to F_y , in the direction

551

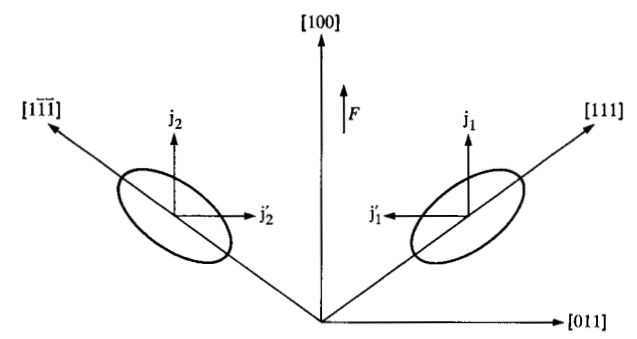


Figure 12 Anisotropic valleys in n-germanium.

of F_{ν} and proportional to it. The second contribution is more complicated. The field F is now oriented so that the conductivity effective mass of electrons in valley 1 is greater than the mass for those in valley 2. The rate at which electrons absorb energy from the electric field, i.e., the rate at which they are heated, is inversely proportional to the conductivity effective mass, so the electrons in valley 2 are heated more than those in valley 1. If the heating rate is large enough there will be a net transfer of electrons by intervalley scattering from the hotter valley to the cooler valley, and the electron population becomes greater in valley 1 than in valley 2. In Eq. (19) the contribution of the two valleys to the y-component of current due to the x-component of field no longer cancel because $n_{\nu}\tau_{\nu}$ is no longer the same in both valleys. There is a contribution j_{xy} to the y-component of current

$$j_{xy} = (\delta n)e\hat{y} \cdot \left(\frac{\overrightarrow{\tau}_1}{m_1} - \frac{\overrightarrow{\tau}_1}{m_2}\right) \cdot \hat{x}F_x. \tag{21}$$

If the constant-energy surfaces have the geometry shown in Fig. 7, characteristic of n-type Ge, j_{zy} is opposite in direction from j_{yy} . So if δn is large enough,

$$j_{\nu} = j_{\nu\nu} + j_{x\nu} < 0, \tag{22}$$

 j_{ν} is oppositely directed from E_{ν} , and we have transverse negative conductivity (TNC).

In n-type Ge the situation exemplified by Fig. 12 is realized when \hat{x} is the [110] direction and \hat{y} the [001]. Valleys 1 and 2 correspond to the valleys lying along the [111] and [11 $\bar{1}$] directions. The other two valleys in the conduction band are normal to the current direction and inactive as far as TNC is concerned. In the presence of TNC, the state with current and field parallel in the [110] direction, one of the three allowed states in Reik and Risken's calculation, is unstable. The field switches to one of the two states with a transverse component of field in the [001] direction.

In his original treatment of this problem, Erlbach thought the intervalley transfer to be too small for the observation of the effect in this orientation. He did observe evidence for the effect with a uniaxial stress applied to eliminate the two unfavorably oriented valleys. Subsequent theoretical work⁴¹ has indicated that transfer by scattering through states in the (100) valleys makes a large contribution to the intervalley transfer and allows the observation of the effect in high electric fields. This larger intervalley transfer also makes the range of current directions around $\langle 110 \rangle$, where the field direction is triple valued, larger than calculated by Reik and Risken, and makes the magnitude of the transverse field larger. Recently Shyam and Kroemer⁴¹ have reported experimental evidence for this effect in strong electric fields at room temperature in unstressed germanium, although a conclusive experimental proof for the existence of this effect has yet to be reported.

That the $\langle 100 \rangle$ minima play an important role in the conductivity of n-Ge in this field range at room temperature had already been demonstrated by the work of Koenig, Nathan, Paul and Smith. In their experiment hydrostatic pressure was used to move the $\langle 100 \rangle$ minima closer in energy to the $\langle 111 \rangle$ minima, and the effects of this motion on the high-field conductivity was studied.

Conclusion

In part I of this review we have discussed the recent developments in the high field conductivity of n-Ge which involve the higher lying $\langle 100 \rangle$ valleys. The instabilities which involve only the $\langle 111 \rangle$ conduction band minima, or which occur in p-Ge, are discussed in II.

References

- J. B. Gunn, Solid State Comm. 1, 88 (1963); also IBM J. Res. Develop. 8, 141 (1964).
- A. A. Kastal'skii and S. M. Ryvkin, Fiz. i Tek. Poluprovodu 1, 622 (1967) [Trans. Soviet Phys.-Semiconductors 1, 523 (1967)].
- J. C. McGroddy and M. I. Nathan, IBM J. Res. Develop 11, 337 (1967).
- 4. J. E. Smith, Jr., Appl. Phys. Letters 12, 233 (1968).
- A. A. Kastal'skii and S. M. Ryvkin, ZhETF Pis. Red.
 446 (1968) [JETP Lett. 7, 350, (1968)] and Proc. IX
 Int. Conf. Physics of Semiconductors, (Moscow 1968),
 955, Nanka, Leningrad (1968).
- E. M. Conwell, Solid State Physics, Supp. 9, Academic Press, 1967.
- 7. E. Erlbach, Phys. Rev. 132, 1976 (1963).
- J. E. Smith, Jr., J. C. McGroddy and M. I. Nathan, IBM J. Res. Develop. 13, 554 (1969, this issue).
- E. J. Ryder and W. Shockley, Phys. Rev. 81, 139 (1951) and E. J. Ryder, Phys. Rev. 90, 766 (1953).
- 10. W. Shockley, Bell Syst. Tech. J. 30, 990 (1951).
- H. Budd, Proc. of the Int. Conf. Physics of Semiconductors (Kyoto, 1966), Phys. Soc. of Japan (Supplement) 21, 420 (1966); T. Kurosawa, ibid., 424 (1966).
- J. Yamashita and K. Inoue, J. Phys. Chem. Solids 12, 1 (1959).

- 13. G. Baraff, Phys. Rev. 128, 2507 (1962), W. P. Dumke, Phys. Rev. 167, 783 (1968).
- 14. J. B. Gunn, J. of Electronics and Control, 2, 87 (1956).
- 15. M. I. Nathan, Phys. Rev. 130, 2201 (1963).
- 16. R. Barrie and R. R. Burgess, Can. J. Phys. 40, 1056 (1962).
- 17. D. Schweitzer and K. Seeger, Z. Physik 183, 2207 (1965).
- 18. B. J. Elliot, J. B. Gunn and J. C. McGroddy, Appl. Phys. Letters, 11, 253 (1967).
- 19. D. M. Chang and J. G. Ruch, Appl. Phys. Letters 12, 111 (1968).
- 20. W. Shockley, Bell Syst. Tech. J. 33, 799 (1954).
- 21. J. C. McGroddy, Proc of the Int. Conf. on Phys. of Semiconductors (Moscow, 1968) p. 984.
- 22. M. H. Jørgensen, N. I. Meyer and K. J. Schmidt-Tiedemann, Proc. 7th Int. Conf. Physics of Semiconductors (Paris 1964) p. 457.
- 23. H. Heinrich and D. K. Ferry, Appl. Phys. Letters 11, 126 (1967).
- 24. See Ref. 6, pp. 34-45, for a discussion of these measurements and references to the original work.
- 25. J. E. Smith, Jr., Phys. Rev. 178, 1364 (1969).
- 25a. J. C. McGroddy, (unpublished results). 26. A. Jayaraman, B. B. Kosicki, and J. C. Irvin, *Phys.* Rev. 171, 836 (1968).
- 27. E. G. S. Paige in Progress in Semiconductors Vol. 8, John Wiley and Sons, Inc. (1964) p. 200.
- 28. J. E. Smith, Jr. and J. C. McGroddy, Appl. Phys. Letters, 11, 372 (1967).

- 29. P. J. Melz and J. C. McGroddy, Appl. Phys. Letters, 12, 321 (1968).
- 30. A. R. Hutson, A. Jayaraman, A. G. Chynoeth, A. S. Coriell, and W. L. Feldman, Phys. Rev. Letters, 14, 639 (1965).
- 31. J. E. Smith, Jr., J. C. McGroddy and M. I. Nathan, Phys. Rev., to be published.
- 32. W. P. Dumke, private communication.
- 33. P. J. Price, to be published.
- 34. R. Stratton, Proc. Roy. Soc. A242, 355 (1957).
- 35. W. Fawcett and E. G. S. Paige, Electronics Letters 3, 505 (1967).
- 36. E. G. S. Paige, IBM J. Res. Develop. 13, 562 (1969, this issue).
- 37. M. Shibuya, Phys. Rev. 99, 1189 (1955).
- 38. W. Sasaki, M. Shibuya, K. Mizuguchi and G. M. Hatoyama, J. Phys. Chem. Solids, 8, 250 (1959).
- 39. V. Dienys and J. Pozhela, Phys. Stat. Sol. 17, 769
- 40. H. G. Reik and H. Risken, Phys. Rev. 124, 777 (1961) and Phys. Rev. 126, 1737 (1962).
- 41. M. Shyam and H. Kroemer, Appl. Phys. Letters, 12, 283 (1968).
- 42. S. H. Koenig, M. I. Nathan, W. Paul and A. C. Smith, Phys. Rev. 118, 1217 (1960).

Received April 11, 1969